Thermochimica Acta, 188 (1991) 63–76
Elsevier Science Publishers B.V., Amsterdam

Calorimetric studies in high resolution DSC systems: identification and simulation by physical models

A. Amengual [1], F. Marco, M. Rodriguez de Rivera [2] and V. Torra

Departamento Fisica Aplicada, ETSAB-ETSECCP, Universitat Politecnica de Catalunya, E-08028 Barcelona (Spain)

(Received 2 January 1991)

Abstract

From the application of identification techniques with a physical image, a model (extended RC at variable temperatures) was made of an actual computer controlled calorimetric system suitable for studying martensitic transformations in shape-memory alloys. A simulation of the behaviour makes it possible to correlate the parameters of the model with the effects that may arise in experimental thermograms. Coherence between the model and the experimental results imposes conditions on the phenomenological interpretation of the transformation, and on some recent interpretations of global energy balance.

INTRODUCTION

The applicability in the robotic domain of shape-memory alloys requires a strict knowledge of the behaviour of the material when subjected to external action. Consider for instance, temperature and/or applied stress [1]. This presupposes knowing the hysteresis cycle and its dependence on and time evolution with temperature and stress [1].

In order to study the hysteresis cycle, in basically stress-free systems, conduction calorimetry (unconventional DSC) is progressively being used [2–5] and provides excellent dynamic information on the transformation. In fact, the thermograms give a direct image of the macroscopic evolution of the material with the cycling and with the characteristics of the thermomechanical treatment [6,7], but they are influenced by the changes in the thermal parameters (heat capacity and heat coupling in the sample) linked to the transformation itself, and also by changes in the parameters of the instrumentation. Furthermore, in the present state of the art, a complete formalism for temperature-dependent calorimetric systems is unavailable.

[1] Permanent address: Departamento de Fisica, Universitat de les Illes Balears, E-07071 Palma de Mallorca, Spain.

[2] Permanent address: Departamento de Fisica, ETSII, Universidad de Las Palmas de Gran Canaria, E-35017 Las Palmas de Gran Canaria, Spain.

0040-6031/91/$03.50

Systematic studies require automatic measuring and data processing systems which make it possible to study the behaviour of shape-memory alloys in relation to time, number of cycles, thermomechanical treatments etc., that is, to carry out a large number of tests under preset temperature programmings, and which do not require constant attention (without quasi-permanent human interaction). Also, these materials usually show fluctuating behaviour due to particular characteristics of each sample (for instance, the grain size in a polycrystal) [8], Thus, systematic studies are necessary to avoid particular results (stochastic effects) in samples or to obtain the average value and the standard deviation. In all, it is necessary to have reliable automated equipment. Thus, a calorimetric system has been developed, which is adapted to the conditions of memory materials [9,10]. A model representation (see, for example, ref. 11 and references cited therein) is also being made of the thermodynamic behaviour of the transformation from calorimetric measurements. In some cases the results are difficult to justify (in the thermodynamic sense) and this makes it necessary to take a new point of view on the calorimetrically measured energies.

In the present paper, by means of simplified modelling (localized constants) of a programmable high-performance calorimetric system and the application of identification techniques with a physical image (see AIRRT in ref. 12), a calculation is made of the more relevant heat parameters (invariant or temperature dependent). This makes it possible to prepare an algorithm for simulating the thermograms and evaluating the behaviour of the device according to the actions produced by temperature programming and, where necessary, the changes associated with transformation and/or its related energy dissipation. Analysis of the numerical results, together with an estimate of the experimental conditions of the martensitic transformations (Cu–Zn–Al alloys), in terms of the first law of thermodynamics makes it possible to establish which parameters are relevant and the most suitable means of analysis for the precise determination of the energy released.

EXPERIMENTAL SET-UP AND MODEL

The experimental system (Fig. 1) is described elsewhere [9,10]. From some Joule effect dissipations, a study was made of the changes in sensitivity and dynamic response vs. temperature (see the values of the first time constant τ_1 in Table 1). This permits us to describe the device in simplified form by means of a non-differential RC model [13,14] (Fig. 2).

In order to obtain satisfactory estimates of the values of heat capacities C_1, C_2 and C_3 and of the heat couplings P_{12}, P_{23}, P_1, P_2 and P_3, we used an automatic identification routine (AIRRT iterative method) which was used in variable mass systems [12]. The method, from an initial model, determines a calculated response and is compared with the experimental thermograms. By successive approximations, the values of the model parameters are

progressively refined. The study of a series of experimental curves associated with different temperatures makes it possible to optimize the values of the heat capacities and couplings and the changes of those that explicity vary with temperature.

The experimental system has two Melcor thermobatteries arranged differentially and the representative model used is non-differential (a single thermobattery). The simulated energy dissipation occurs in the first element and the response model corresponds to the difference $T_2 - T_3$ (Fig. 2 (left)).

The energy balance applied to each model element enables us to write

$$W(t) = C_1 \, dT_1/dt + P_{12}(T_1 - T_2) + P_1(T_1 - T^*)$$

$$P_{12}(T_1 - T_2) = C_2 \, dT_2/dt + P_{23}(T_2 - T_3) + P_2(T_2 - T^*)$$

$$P_{23}(T_2 - T_3) = C_3 \, dT_3/dt + P_3'(T_3 - T_0) + P_3''(T_3 - T^*)$$

By rearranging the preceding system we obtain

$$W(t) = C_1 \, dT_1/dt + P_{12}(T_1 - T_2) + P_1(T_1 - T^*)$$

$$0 = C_2 \, dT_2/dt + P_{12}(T_2 - T_1) + P_{23}(T_2 - T_3) + P_2(T_2 - T^*)$$

$$0 = C_3 \, dT_3/dt + P_{23}(T_3 - T_2) + P_3'[T_3 - T^* - (T_0 - T^*)] + P_3''(T_3 - T^*)$$

Taking T^* as the origin of the temperatures we are left with

$$W(t) = C_1 \, dT_1/dt + P_{12}(T_1 - T_2) + P_1 T_1$$

$$0 = C_2 \, dT_2/dt + P_{12}(T_2 - T_1) + P_{23}(T_2 - T_3) + P_2 T_2$$

$$P_3'(T_0 - T^*) = C_3 \, dT_3/dt + P_{23}(T_3 - T_2) + P_3 T_3$$

The above system, with the aid of the AIRRT algorithm, enables us to determine the values of the parameters and their dependence on temperature (Tables 1 and 2). The curves simulated by the model and the experimental curves begin to diverge from the fourth significant figure. The parameters were determined for different working temperatures, assuming $T_0 = T^*$.

SIMULATION AND NUMERICAL VS. EXPERIMENTAL RESULTS

From the numerical values of the parameters, a simulation can be made of the thermograms associated with the effects of temperature programming, dissipated power and, if necessary, by introducing other changes, either independent or correlated. We integrated the previous equations with the aid of the Runge–Kutta method of the IBM Scientific Subroutine Package, and they were adapted to take into account the various possibilities of changes in the parameters. For example, we can simulate the evolution of the heat capacity by the phase change or the changes in coupling by alterations in the

surface roughness with the transformation. Introducing the ΔP and ΔC changes, from the preceding system we obtain

$$W(t) = (C_1 + \Delta C)\, dT_1/dt + (P_{12} + \Delta P)(T_1 - T_2) + P_1 T_1$$

$$0 = C_2\, dT_2/dt + (P_{12} + \Delta P)(T_2 - T_1) + P_{23}(T_2 - T_3) + P_2 T_2$$

$$P_3'(T_0 - T^*) = C_3\, dT_3/dt + P_{23}(T_3 - T_2) + P_3 T_3$$

From the indetermination of the experimental data for P_3', $P_3' = P_3$ is assumed. The preceding system can be written as

$$W(t) - \Delta C\, dT_1/dt - \Delta P(T_1 - T_2) = C_1\, dT_1/dt + P_{12}(T_1 - T_2) + P_1 T_1$$

$$\Delta P(T_1 - T_2) = C_2\, dT_2/dt + P_{12}(T_2 - T_1) + P_{23}(T_2 - T_3) + P_2 T_2$$

$$P_3(T_0 - T^*) = C_3\, dT_3/dt + P_{23}(T_3 - T_2) + P_3 T_3$$

With this structure, C_1 and P_{12} would be the values in the β or austenite phase, and ΔC and ΔP would be the changes associated with the progressive transformation of the sample into the other phase (martensite). The previous equations show that the effects of temperature programming $P_3(T_0 - T^*)$ and of ΔC and ΔP are equivalent to some additional and disturbing dissipations of the energy response of the "pure transformation" or $W(t)$.

In the case of the model of four capacities, involving a transformation of the material differentiated into two parts (transformation in the first element and the ΔC and ΔP effects in the second), the representative equations take the form

$$W(t) = C_1\, dT_1/dt + P_{12}(T_1 - T_2) + P_{13}(T_1 - T_3) + P_1 T_1$$

$$\Delta C_2\, dT_2/dt + \Delta P_{23}(T_3 - T_2) - \Delta P_2 T_2$$
$$= C_2\, dT_2/dt + P_{12}(T_2 - T_1) + P_{23}(T_2 - T_3) + P_2 T_2$$

$$\Delta P_{23}(T_2 - T_3) = C_3\, dT_3/dt + P_{23}(T_3 - T_2) + P_{34}(T_3 - T_4) + P_{13}(T_3 - T_1) + P_3 T_3$$

$$P_4(T_0 - T^*) = C_4\, dT_4/dt + P_{34}(T_4 - T_3) + P_4 T_4$$

The choice of the numerical values of the parameters was made from the model of three elements with the conditions

$$C_1(4) + C_2(4) = C_1(3); \quad C_3(4) = C_2(3); \quad C_4(4) = C_3(3);$$
$$P_1(4) + P_2(4) = P_1(3); \quad P_3(4) = P_2(3); \quad P_4(4) = P_3(3);$$
$$P_{13}(4) + P_{23}(4) = P_{12}(3); \quad P_{34}(4) = P_{23}(3)$$

Some simulations were made assuming that the variations of the parameters ΔC and ΔP are correlated with the energy released by the sample. In this case we are associating ΔC and ΔP with the change in the "transformed material", and it is assumed that the energy is proportional to the mass transformed. The variation of the heat coupling associated with changes

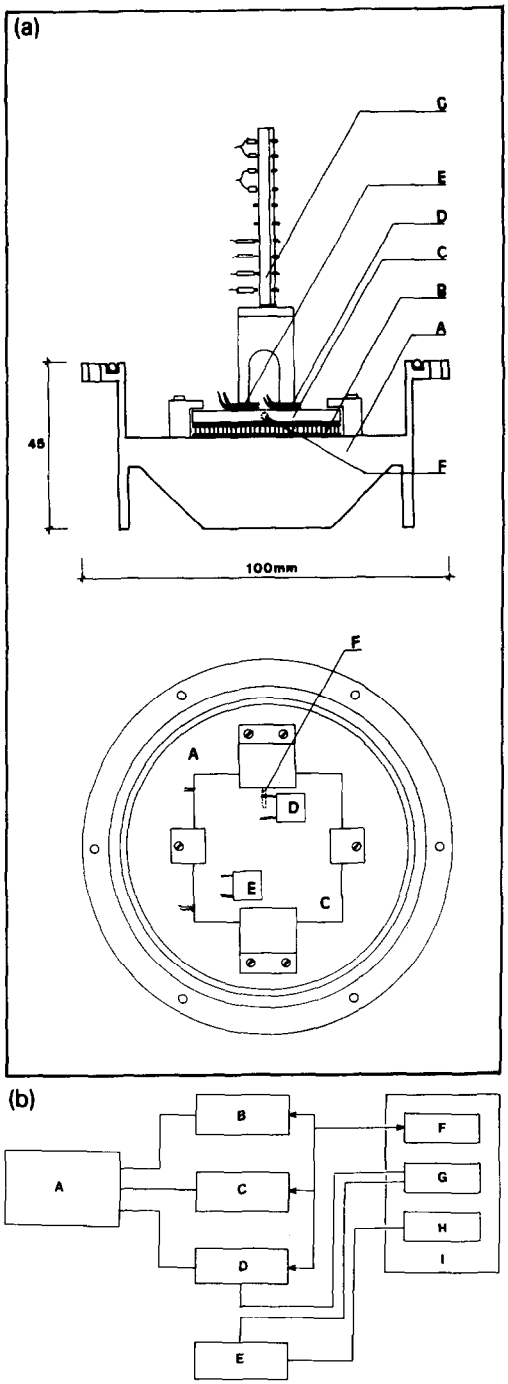

Fig. 1. (a) Experimental set-up: A, brass block immersed in a thermal bath; B, Peltier thermobattery; C, working space at a regulated temperature; D and E, calorimetric thermobatteries (Seebeck effect); F, resistance Pt-100; G electrical links. (b) Block diagram: A, experimental set-up; B, resistance measurement $R(t)$ with DMM HP3478A; C, thermogram $s(t)$ with DMM HP3478A; D, Peltier effect $I(t)$ with DMM HP3478A; E, power supply (Premium SR-120); F, GPIB board; G, switching board; H, digital/analogue converter (board: ADDA 14); I, PC-XT computer.

TABLE 1

Model of the three elements: experimental sensitivity (SENS) and first time constant τ_1 vs. temperature, and evolution of P_3 and P_{23} with temperature

T (°C)	τ_1 (s)	SENS (mV W^{-1})	P_3 (W K^{-1})	P_{23} (W K^{-1})
−40.53	6.4	277.5	0.033768	0.068838
−27.91	–	292.25	0.033173	0.062279
−17.78	6.9	304.2	0.033695	0.061898
−15.24	6.9	307.1	0.033487	0.061109
0.0	7.2	324.1	0.034087	0.059033
23.11	7.7	346.5	0.032734	0.051252
43.78	8.3	362.2	0.034724	0.047263
54.16	8.4	368.2	0.034474	0.045703
64.58	–	371.9	0.034453	0.044774

in the thermal resistance are linked to the change in surface texture of the sample by the appearance of the different self-accommodated variants of martensite [15]. We shall also assume this variation to be proportional to the energy released.

The thermograms are determined for different temperature programmings. Figure 3 shows a linear programming where the rate of temperature change (dT_0/dt) is constant and ΔC_2 is proportional to the energy that is being released. In this case, a determination of the value of the corrected thermogram (by inverse filtering) from the steady state enables us to

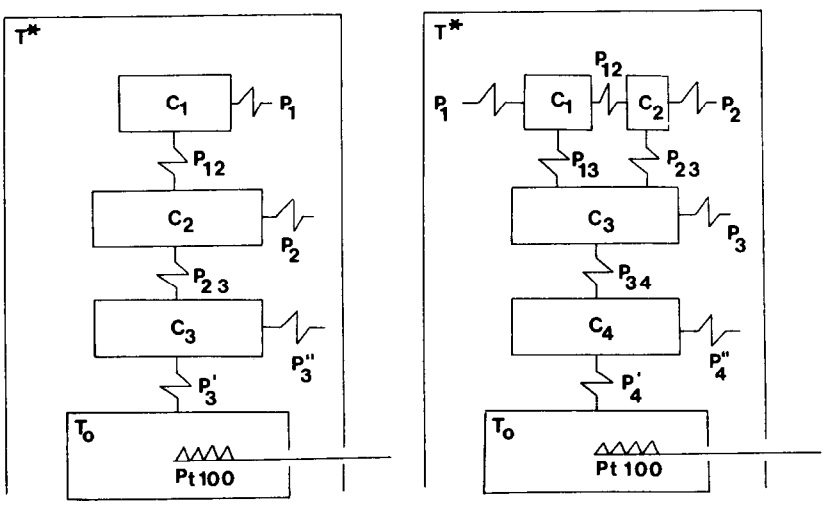

Fig. 2. *RC* model (non-differential calorimeter): C_i are the heat capacities, P_{ij} and P_i the thermal couplings, T_0 is the programmed temperature and T^* is the thermal bath temperature. A Pt-100 resistance is used in the temperature control device. In a four-elements model, C_1 is decomposed into two heat capacities with appropriate thermal couplings (see Table 2).

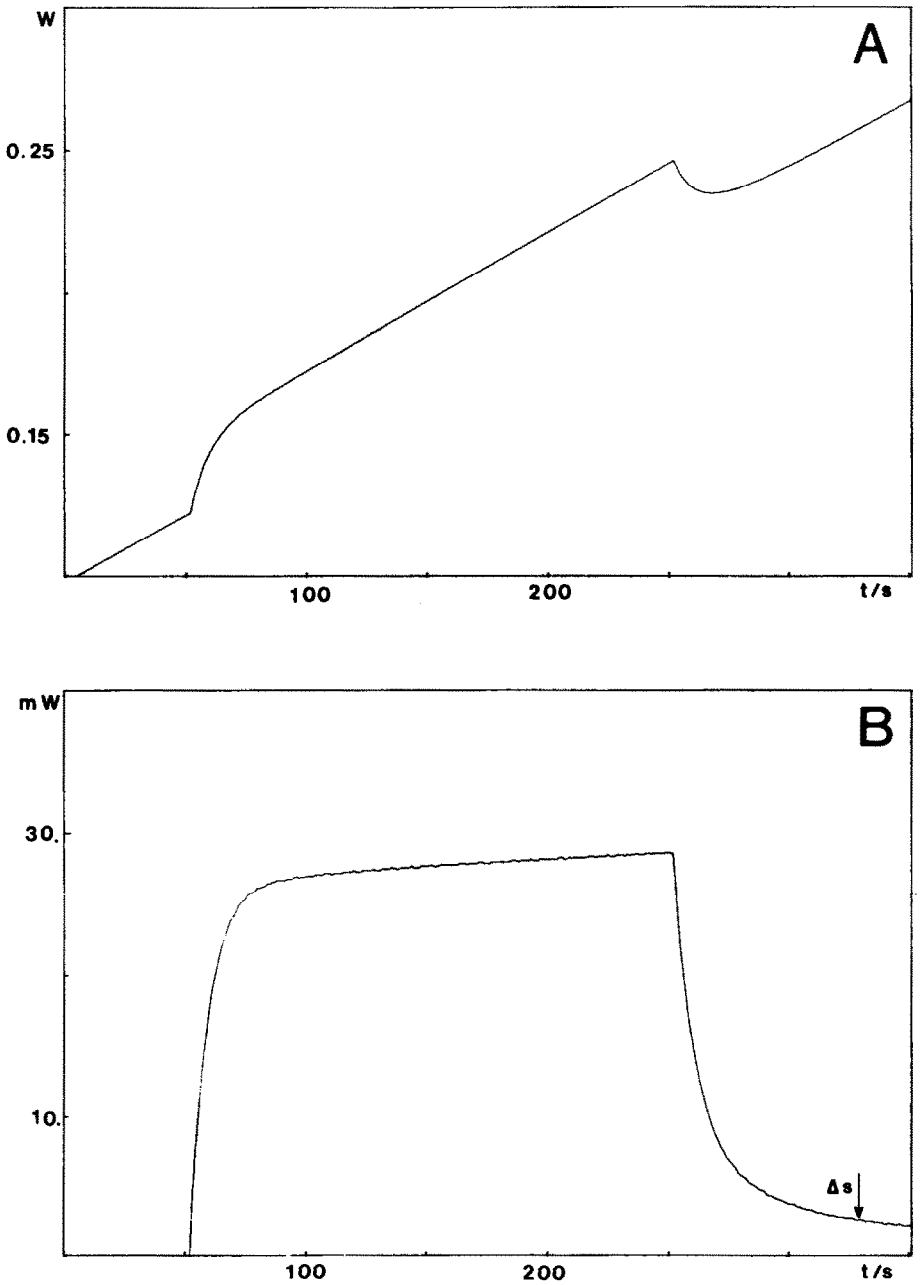

Fig. 3. Calculated thermograms using the four-elements model: heating with a step signal of 27 mW during 200 s; temperature programming with. $T_0 = 5.9636 - 0.0095t$ (T_0 in degrees Celsius and t in seconds); the bath temperature is $T^* = 8°C$, $\Delta C_z(t) \propto \int W dt$. A, calculated thermogram; B, calculated thermogram without baseline.

TABLE 2

Automatic identification (AIRRT): values of C_i (heat capacities (J K^{-1}) and P_{ij} and P_i (thermal couplings (W K^{-1})); (VAR) = temperature-dependent parameter

Three heat capacities model, heating in C_1, output thermogram		
$s(t) \propto T_2 - T_3$		
$C_1 = 0.80000$	$P_1 = 0.05000$	$P_{12} = 17.505$
$C_2 = 0.65000$	$P_2 = 0.6E\text{-}05$	$P_{23} = 0.068838$ (VAR)
$C_3 = 0.96711$	$P_3 = 0.033768$ (VAR)	
Four heat capacities model, heating in C_2, output thermogram		
$s(t) \propto T_3 - T_4$		
$C_1 = 0.72000$	$P_1 = 0.04500$	$P_{12} = 0.1200$
$C_2 = 0.08000$	$P_2 = 0.00500$	$P_{13} = 15.7545$
$C_3 = 0.65000$	$P_3 = 0.6E\text{-}05$	$P_{23} = 1.7505$
$C_4 = 0.96711$	$P_4 = 0.033768$ (VAR)	$P_{34} = 0.068838$ (VAR)

differentiate approximately the energy contributions to $W(t)$ and to the term $\Delta C_2 \mathrm{d}T_2/\mathrm{d}t$ by

$$\Delta C_2 \, \mathrm{d}T_2/\mathrm{d}t = \Delta s \approx \Delta C_2 K_c \, \mathrm{d}s/\mathrm{d}t$$

K_c is a parameter of the device, and the correction Δs, when $\mathrm{d}s/\mathrm{d}t$ and $\mathrm{d}T_2/\mathrm{d}t$ are constant, can be seen in Fig. 3.

Figure 4 (A and B) shows an experimental thermogram resulting from heating (or cooling) a sample of Cu–Zn–Al by means of constant temperature rate programming. This thermogram, relating to a spontaneous transformation, shows a change in direction of the baseline before and after transformation, but without an apparent shift in the baseline. This shows us that the experimental response does not correspond to the previous simulations (permanent changes in ΔC and ΔP parameters). Furthermore, all the interpretations—experimental and model—indicate that there does not appear to be a relevant change in the specific heat of the material with the transformation [15].

Despite this, in the literature there appear remarkable differences in the energies measured in transformation and in retransformation (over 50% in Fig. 2 of ref. 11). Usually, the energies measured are determined from conventional baselines drawn under the dissipation area. For example, the energies measured under the energy pulses of the thermogram in Fig. 6 are found in Table 3 and there are some remarkable differences (near 11%) between transformation and retransformation.

These differences are difficult to interpret since for cyclic behaviour they correspond to a heat absorption and as a result a work production with an output of up to 50%. Since the width of the cycle associated with the hysteresis involves differences below 10 K (mean temperature, nearly 250 K in ref. 11), the maximum theoretical output of a Carnot machine cannot exceed 4%. In the case of Fig. 6, it cannot exceed 0.1%. In all cases the

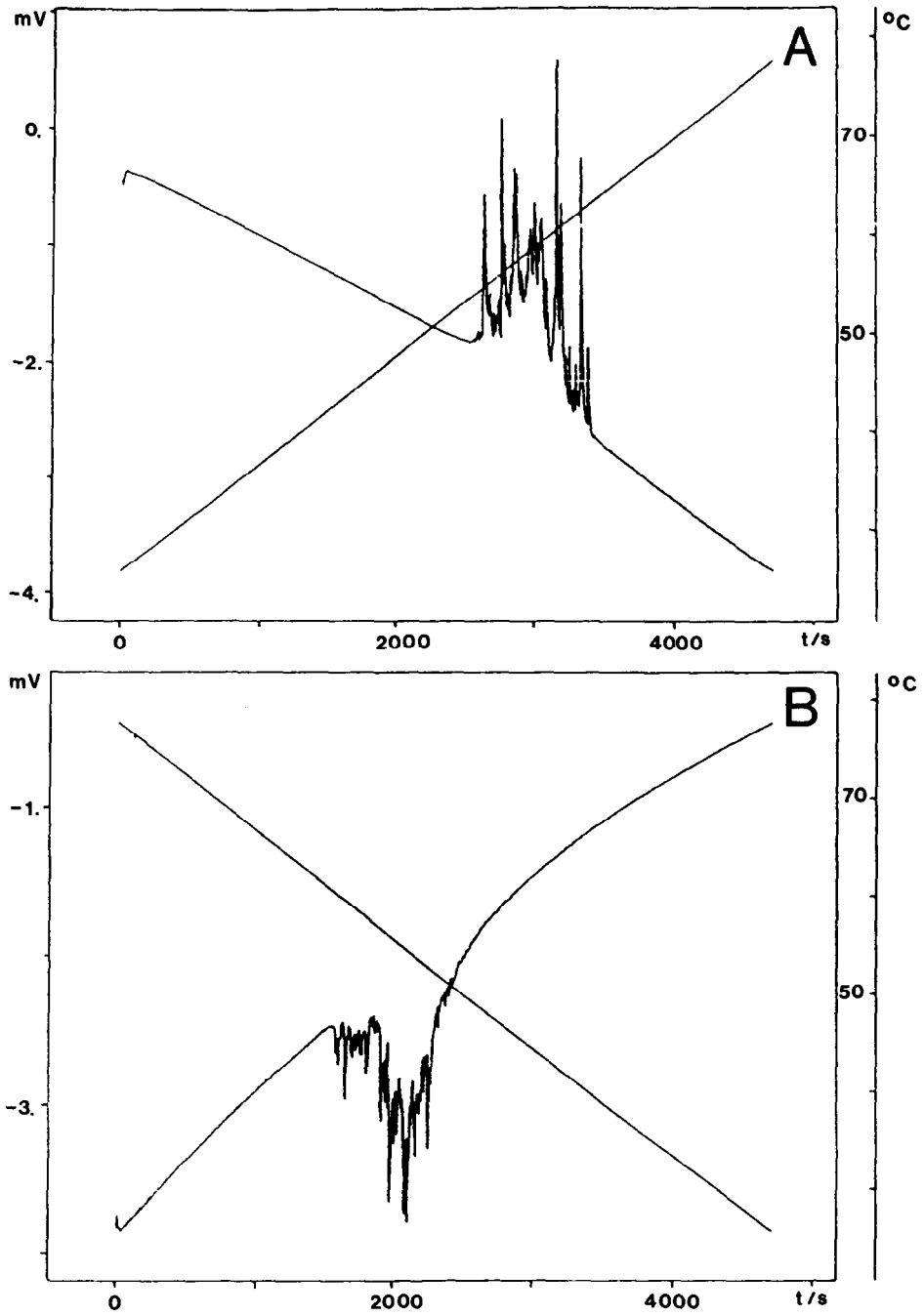

Fig. 4. Experimental thermograms in a martensitic transformation (Cu–Zn–Al shape-memory alloy, from ref. 16): A, heating; B, cooling.

TABLE 3

Enthalpy changes (mJ) in austenite to martensite $\beta \rightarrow M$ or in the reverse process $M \rightarrow \beta$: (A) standard baseline; (B) linking same temperature points

	Cooling	Heating	Cooling	Heating	Cooling	Heating
(A)	−14.6	16.3	−15.1	16.6	−15.2	17.0
(B)	−28.6	28.1	−23.0	25.7	−25.2	24.6

second law of thermodynamics indicates that the energy differences over the Carnot cycle are erroneous.

The thermodynamic conditions show us that without relevant external mechanical work, and if the state of the material in a complete transformation cycle does not vary, the equation $\Sigma Q_i = 0$ should be true.

Obviously, the choice of baseline is extremely critical for estimating the energy balance and requires a choice appropriate to the type of phenomenon. In our case, we could assume that before beginning the transformation there is a progressive release of energy until the area affected transforms. Therefore, the total transformation energy would be split into two parts:

$$\Delta H = \Delta H' + \Delta H''$$

The $\Delta H'$ is dissipated from T_E (equilibrium temperature) to T'_E, at which temperature the material transforms, releasing $\Delta H''$. Attempts using $\Delta C = d\Delta H'/dT_2$ (the model with four heat capacities) appear more coherent with the experimental observations. The simulation made for constant temperature rate programming is found in Fig. 5. Here, it is clearly shown that the effect of ΔC on the thermogram is the same as that which occurs when an approximately constant power is dissipated. In fact

$$\Delta C\, dT_2/dt = (d\Delta H'/dT_2)(dT_2/dt) = d/dt(\Delta H')$$

In Fig. 5, it is seen that it is clearly wrong to take as a baseline a line joining the points (a) and (b). This would give a measurement of energy released lower than that which really occurred.

The study of a partial transformation involving a very small (about 400 μm) and stress-free shift of a single interphase β–M, for a very restricted temperature interval (0.4 K), was made by means of sinusoidal programming [16]. The corresponding thermogram, after the elimination of the effect of the sinusoidal programming, is shown in Fig. 6. By taking identical points at the same temperature, the baseline can be drawn, and in this way the same energies can be obtained—in absolute figures—in the transformation ($\beta \rightarrow$ M) as in the retransformation ($M \rightarrow \beta$) (see Table 3).

Expansion of the thermograms, together with microscopic observation of the movement of the interphases vs. time, appears to suggest the presence of a specific heat abnormality associated with metastable states before transformation and retransformation. In fact, in these cycles there are asymmetries

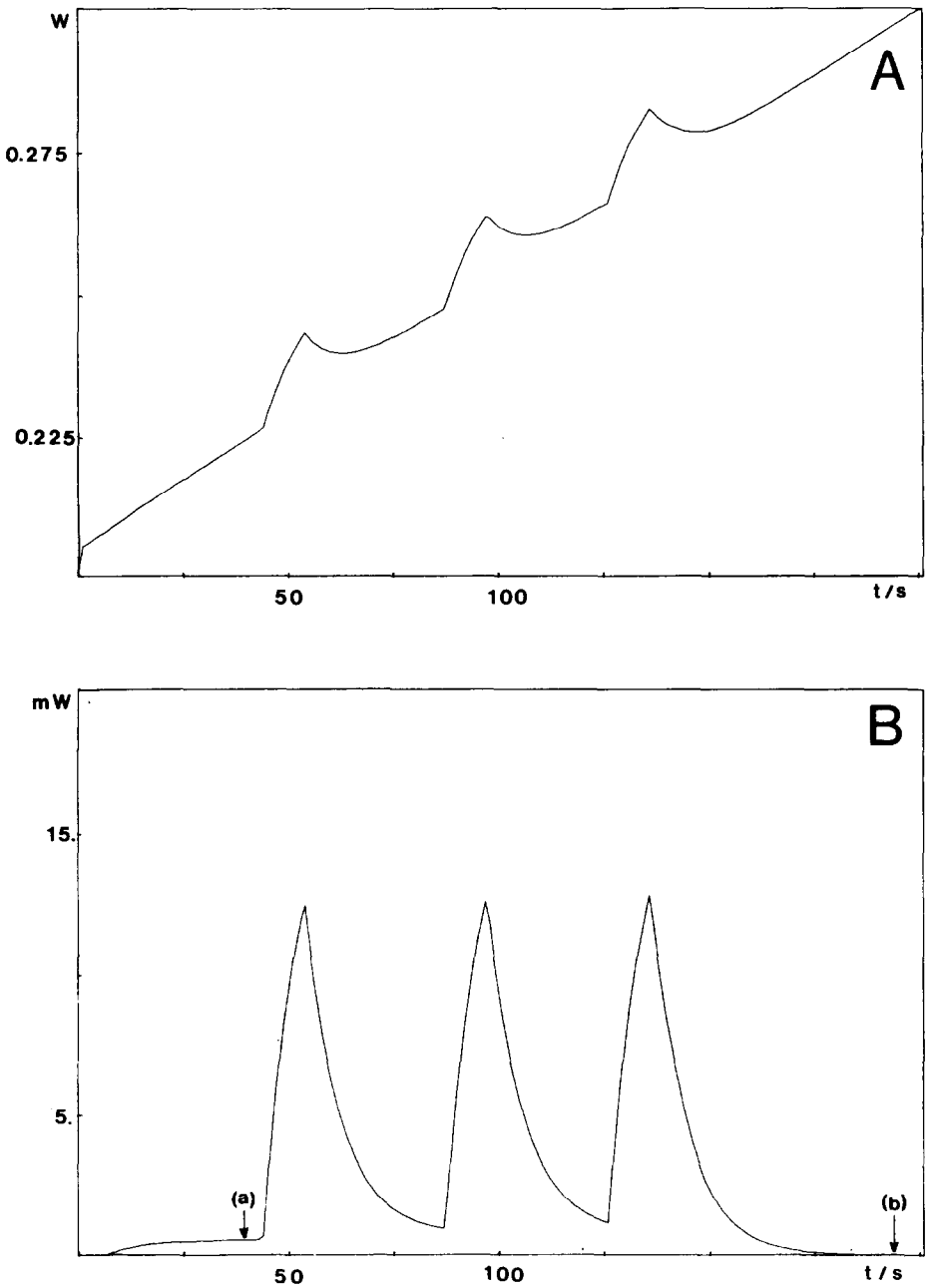

Fig. 5. Calculated thermograms using the four-elements model: heating with a three-step signal (each of 18 mW during 10 s); temperature programming with $T_0 = 3.827 - 0.0095\ t$ (T_0 in degrees Celsius and t in seconds); the bath temperature is $T^* = 8\,^\circ C$; $\Delta C_2(t) = 0.2\ J\ K^{-1}$ (metastability action) in the temperature range $6.55 < T_2 \leqslant 6.85\,^\circ C$. A, calculated thermogram; B, calculated thermogram without baseline; In zone (a) the metastability action is observed.

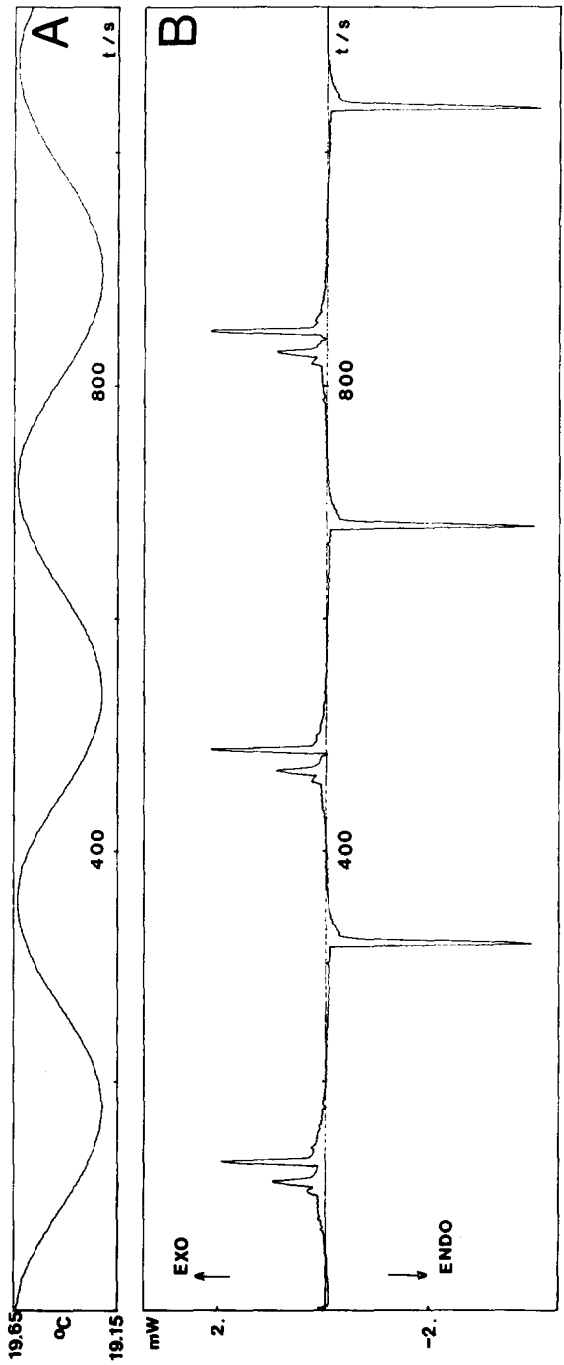

Fig. 6. Stress-free transformation of a single interface calorimetric measurement (ref. 16): A, temperature programming; B, experimental thermogram after numerical filtering in heat power units (mW).

in the hysteresis cycle described in terms of the amount of martensite measured by optical microscopy [16]. All this suggests that metastability is extended to the rest of the sample that has not yet been transformed. In the retransformation processes, the metastability remaining in partial transformation progressively disappears as the temperature rises and requires an additional contribution of energy. This process is repeated in every temperature programming period.

CONCLUSIONS

The AIRRT approach enables us to estimate the parameters of the system and in particular those that have a relevant variation with temperature.

From a comparison between the thermograms and the results of the model, it can be shown that there is no relevant effect of ΔC and ΔP with transformation to explain the enthalpy differences between transformation–retransformation processes.

The differences reported in the literature between the energies measured in transformations and retransformations may be associated with uncertainties in the estimate of the baseline owing to the existence of metastability between the two phases. To interpret actual systematic differences in the heating–cooling processes, only internal energy differences seem realistic: for instance, differences related to stabilization processes in the martensite phase and/or ordering phenomena in the β phase.

ACKNOWLEDGEMENTS

Financial support from CICYT projects 86-0079 and MAT89-0407-C03 and EURAM 0803/3 MA1E-0010-C (GDF) are gratefully acknowledged.

REFERENCES

1 Science and technology in shape memory alloys, Proc. COMETT Course, V. Torra (Ed.), Univ. Illes Balears, Mallorca, 1990, pp. 4–6.
2 H. Tachoire, J.L. Macqueron and V. Torra, in M.A.V. Ribeiro da Silva (Ed.), Thermochemistry and its Applications to Chemical and Biochemical Systems, NATO Ser. C, Vol. 119, Reidel, Dordrecht, 1984, pp. 77–126.
3 C. Picornell, C. Seguí, V. Torra, J. Hernáez and C. López del Castillo, Thermochim. Acta, 91 (1985) 311.
4 H. Tachoire, J.L. Macqueron and V. Torra, Thermochim. Acta, 105 (1986) 333.
5 J. Van Humbeeck, D. Van Hulle, L. Delaey, J. Ortín, C. Seguí and V. Torra, Trans. Jpn. Inst. Met., 28(5) (1987) 383.
6 C. Picornell, C. Seguí, V. Torra, C. Auguet, Ll. Mañosa, E. Cesari and R. Rapacioli, Thermochim. Acta, 106 (1986) 209.
7 C. Picornell, C. Seguí, V. Torra and R. Rapacioli, Scr. Metall., 22 (1988) 999.
8 J.M. Guilemany, personal communications, 1989.
9 A. Amengual and V. Torra, J. Phys. E, 22 (1989) 433.

10 V. Torra and H. Tachoire, J. Therm. Anal., 36 (1990), 545.
11 A. Planes, J.L. Macqueron and J. Ortin, Philos. Mag. Lett., 57(6) (1988) 291.
12 M. Rodriguez de Rivera, F. Socorro, J.P. Dubés, H. Tachoire and V. Torra, Thermochim. Acta, 150 (1989) 11.
13 J.L. Macqueron, J. Navarro and V. Torra, An. Fis., 73 (1977) 163.
14 W. Zielenkiewicz (Ed.), Thermokinetics. Signal Processing in Calorimetric System, Ossolineum, Warsaw, 1990.
15 M. Ahlers, Prog. Mater. Sci., 30 (1986) 135.
16 A. Amengual, Doctoral Thesis, Universitat de les Illes Balears, Mallorca, 1990.